

Magnetostriction of grain oriented Si-Fe and its domain model

Abstract. Transformer noise has been drawing more and more attentions recently. One of the main causes of transformer noise is magnetostriction of grain oriented electrical steel sheets. Magnetostrictions perpendicular to the rolling direction should also be focused in addition to those to the rolling direction, because magnetic flux flows out of the rolling directions especially around T-joint parts of 3-phase transformers. In this paper, magnetostrictions of high permeability grain oriented electrical steel sheets to the both directions were measured with a Doppler-vibrometer and rationalized by magnetic domain models.

Streszczenie. Szumy generowane przez transformatory są obecnie analizowane coraz bardziej szczegółowo. Głównym ich źródłem jest magnetostrykcja blach zorientowanych. Magnetostrykcja prostopadła do kierunku walcowania powinna być także brana pod uwagę ponieważ strumień magnetyczny nie zawsze jest w kierunku walcowania. W artykule przeanalizowano magnetostrykcję blach zorientowanych w obu kierunkach używając wibrometr Dopplera. (**Magnetostrykcja blach anizotropowych SiFe i jej model domenowy**)

Keywords: grain oriented electrical steel, magnetostriction, magnetic domain

Słowa kluczowe: blachy anizotropowe, magnetostrykcja, domeny magnetyczne

Introduction

Grain oriented electrical steel sheets (GO) are mainly used for transformer cores of commercial frequencies, 50Hz or 60Hz. Most required property for transformers is lower loss, and GO with lower iron loss have been always sought for. In addition, recently, smaller transformer noise is strongly required according to the growing consciousness on environment, especially for transformers installed in city neighbors. Magnetostriction of GO is one of the largest origins of transformer noise and has been measured and analyzed by many researchers [1-4].

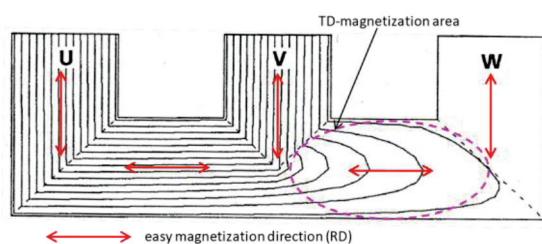


Fig.1. FEM-calculation of flux lines in a 3-phase transformer core.

GO sheets are laminated as the rolling directions, or the high permeability directions, parallel to the longer sides of yokes and limbs of transformers. And magnetostrictions to the rolling directions are primarily related to transformer noises. Even though, some parts of transformer cores are magnetized out of the rolling directions of GO, especially at yokes around T-joint parts of 3-phase transformer cores, as shown in figure 1. As a result, magnetostrictions when magnetized out of the rolling directions are also related to transformer noises.

Experimental procedures

0.23mm-thick grain oriented electrical steel sheets with high permeability were prepared. 100 x 500mm size samples were shear-cut for magnetostriction measurement. The longer sides of several samples were along the rolling direction, RD-samples, and the longer sides of several samples were perpendicular to the rolling direction, TD-samples. All the samples are as prepared and no stress relief annealing was processed.

The block diagram of magnetostriction measuring system is shown in figure 2 [5]. One sample end is clamped, and a small weight reflector is pasted on the other end of a sample. The distance between the clamp and the reflector is 270mm. A sample is magnetized alternatively by an exciting coil, and magnetostrictive vibration velocity is

measured with a Doppler-vibrometer. Magnetostrictive displacement is measured by integration of the magnetostriction vibration velocity. The Doppler-vibrometer is differential type, and inevitable vibration of the magnetizing frame is subtracted by referencing vibration from a reflector pasted on the frame, or external vibration noises are reduced.

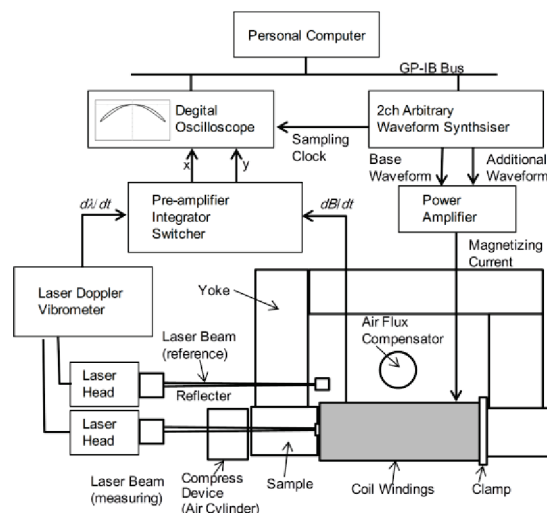


Fig.2. Block-diagram of magnetostriction measuring system.

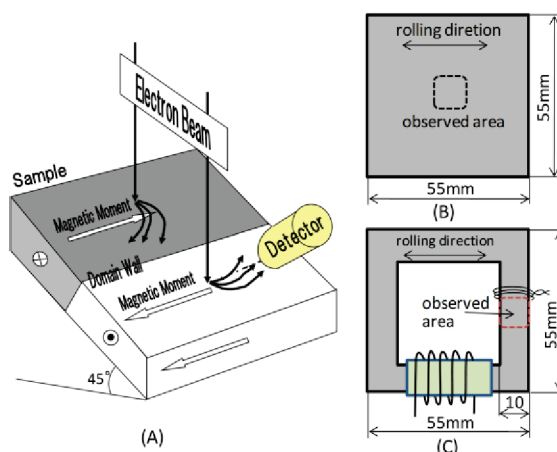


Fig.3. (A) Schematic illustration of Lorentz SEM type-2 contrast, (B) Square sample, (C) Hollow square sample.

Magnetic domains were observed with a Lorenz SEM using type-II contrast [6]. Figure 3 is a schematic illustration of type-2 contrast mechanism. Backscattered electrons are deflected to opposite directions by the domains intersected by a 180-degree domain wall because of Lorenz-force. When an electron detector is arranged properly, magnetic domain contrast emerges. Acceleration voltage of this Lorenz-SEM is 200kV, high enough to observe magnetic domains under insulation coatings and forsterite films, because the electrons have sufficient energy to penetrate them. A 55mm square sample and a 55mm hollow square sample were cut and annealed at 1073K for 2 hours for stress relief. The square sample was magnetized with an external magnetizing yoke equipped to a sample holder. The hollow square sample was magnetized with magnetizing coils directly wound to the sample.

Results and discussions

1). Magnetostriction to RD

Measured magnetostriction data to RD are shown in figure 4. Lissajous curves of magnetostriction to RD in vertical axes and flux density to RD in horizontal axes are drawn under sinusoidal magnetization. These curves are usually called as "butterfly curves". Peak magnetic flux density was varied from 1.3T to 1.9T. Magnetostrictions of high permeability GO are usually very small in RD, typically below 0.3×10^{-6} in amplitude even at high peak flux density. GO sheets deform in a somehow complicated way when magnetized. At first, GO sheets are contracted to flux density around 1.75T, and then elongated at higher flux density. The magnetostrictive deformations differ at ascending magnetization and at descending magnetization, showing hysteresis, especially at 1.9T peak flux density.

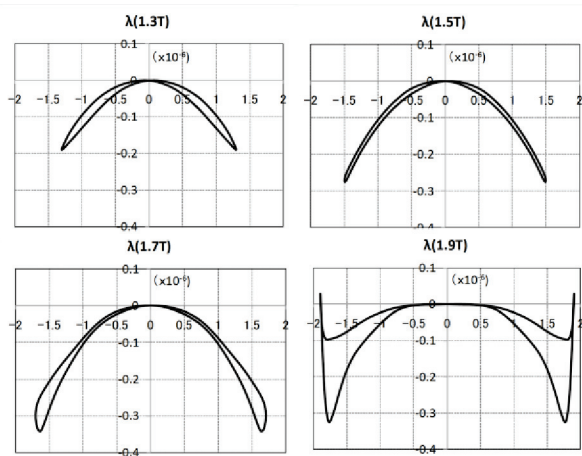


Fig.4. Measured butterfly curves of high permeability GO at 50Hz - sinusoidal magnetization to RD.

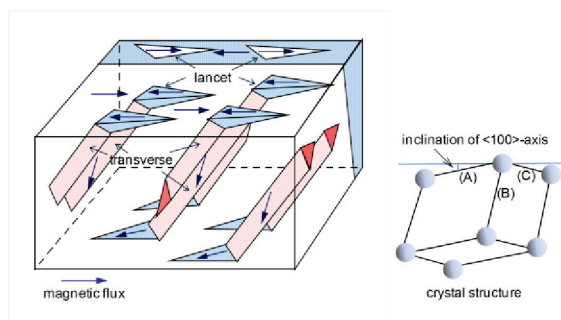


Fig.5. Schematic illustration of "lancets" and inner domain structures.

This magnetostriction behavior could be explained by a magnetic domain model. Generally, Fe-based materials including electrical steel sheets are magnetized to <100> easy magnetization axes, because of the strong crystal anisotropy. First, slab-shape main domains and having magnetizations aligned to <100>-axes of smallest angle with the sheet surface appear. Main domains are divided by 180-degree domain walls and change magnetization directions by 180-degrees at the walls. Driving force of this division is mainly the stray field energy from surface magnetic charges caused by small inclinations of <100>-axes. Secondly, further reduction of stray field energy is realized by the emergence of triangle shape "lancets" [8]. Inner domain structures under lancets are illustrated schematically in figure 5. These inner domain structures consist of surface domains and transverse domains. The transverse domains are magnetized to <100>-axes intersecting the surface with an angle of 45-degree, as denoted B or C in figure 5.

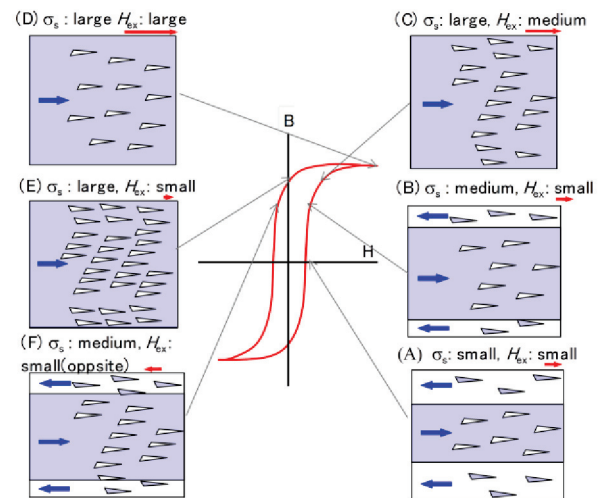


Fig.6. Magnetization by main domain wall displacement and creation and annihilation of "lancets" under alternative magnetization.

Saturation magnetostriction λ_{100} to <100>-direction is 2.18×10^{-5} for 3%Si-Fe. demagnetized state as a reference [9]. It means that GO sheets are elongated as $3/2\lambda_{100}$, or 3.27×10^{-5} , in each of main domains. Magnetization of GO sheets occurs by main domain wall displacement. No magnetostrictive deformation should appear by the main domain wall displacement, because all the domains are elongated to the same direction. During magnetization, lancet distribution densities are also changed due to the stray field energy modification by main domain wall displacement (figure 6). Inner domain structures of lancets comprise transverse domains elongated at the right angle to RD, and the increase of lancets induces the contraction to RD. Lancet distribution densities should also be influenced by external field. Comparing (B) and (F) in figure 6, stray field energy from main domains is the same. Although Zeeman energy with external fields are different, and transverse domains in (B) has larger energy than in (F). Therefore lancets are suppressed in (B), and the lancet distribution density is smaller in (B) than in (F), and so is the contraction to RD. The situation is the same in (C) and (E). This difference in lancet distribution density is considered to be the mechanism of hysteresis in butterfly curves when magnetized to RD. The alternation of lancet distribution density is confirmed by Lorenz-SEM observation as shown in figure 7.

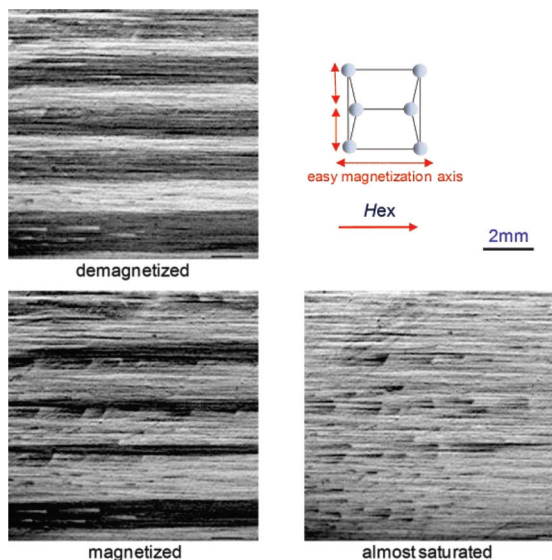


Fig.7. Observed domain images by 200kV-Lorenz SEM, when magnetized by DC-field to RD.

Lancet distribution density can be calculated as a function of the inclination angle of $\langle 100 \rangle$ -axis from the surface plane, assuming a simplified "lancet comb" structures [10]. Transverse domain volume fraction under lancet combs decreases as the $\langle 100 \rangle$ -axis inclination angle decreases and disappears below certain critical values. Higher permeability GO sheets have statistically smaller $\langle 100 \rangle$ -axis inclination angles and should have smaller transverse volume fraction. This calculation would well explain our experiences, that higher permeability GO sheets have smaller magnetostrictions in general.

It is also calculated that applied tensile stress to GO sheets should suppress lancets and consequently transverse domain volume fraction. GO sheets are usually applied tensile stress from insulation coatings and forsterite films [11] and the applied tensile stress would be effective to reduce magnetostrictions of GO sheets.

GO sheet thickness should have some effect on lancet density. In thinner GO sheets, lancet comb distribution density would be somehow smaller and so the transverse volume fraction and magnetostriction.

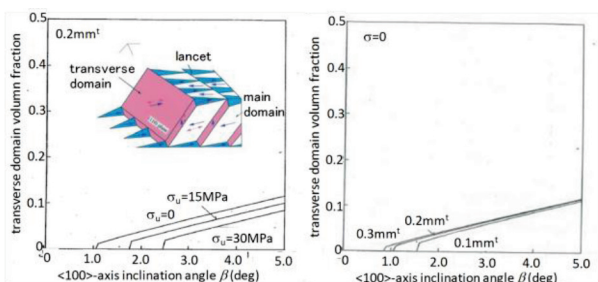


Fig. 8. Calculated transverse domain volume as a function of inclination angle of $\langle 100 \rangle$ -axis from the surface plane. (A).Applied uniaxial tensile stress is varied. (B).GO sheet thickness is varied.

2). Magnetostriction to TD

Measured butterfly curves of TD-magnetization and TD-magnetostriction are shown in figure 8. Peak flux density was varied from 0.6T to 1.6T. Magnetostrictions to TD are almost two-order larger than those to RD. GO sheets are elongated monotonically to 19×10^{-6} at 1.4T flux density and then slightly contracted at 1.6T. Butterfly curves to TD show no hysteresis, not as those to RD.

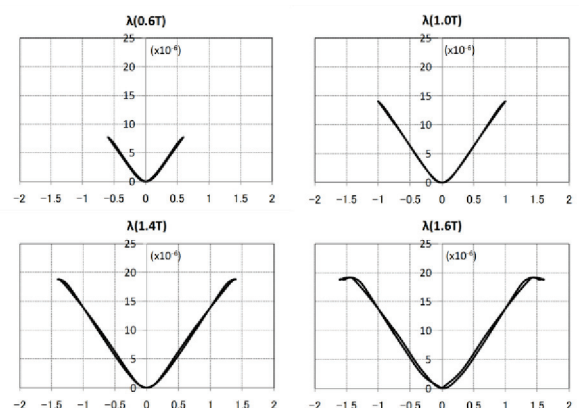


Fig.9. Measured butterfly curves of high permeability GO at 50Hz-sinusoidal magnetization to TD.

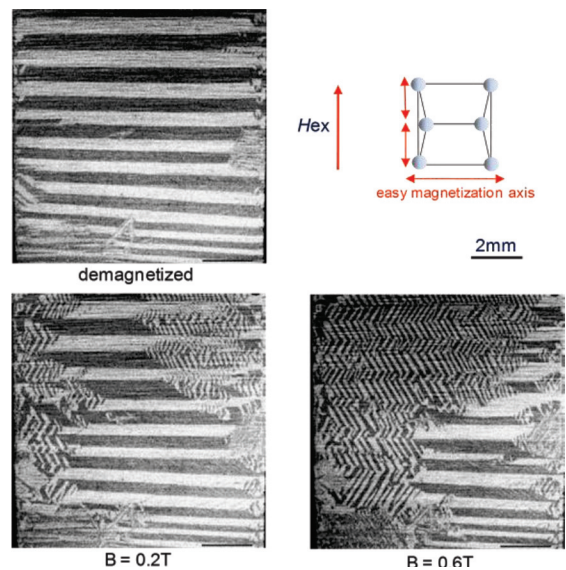


Fig.10 Observed domain images by 200kV-Lorenz SEM, when magnetized by DC-field to TD.

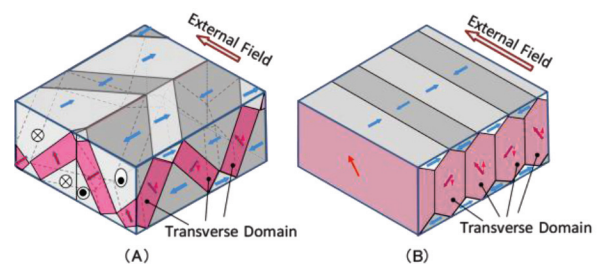


Fig.11. Schematic illustrations of (A) "saw-tooth" patterns, (B) "column" patterns and inner domain structures.

The magnetostriction behavior to TD could also be explained by a domain model. No domain images were observed in a square sample magnetized to TD. It means that the magnetization directions of surface domains were perpendicular to the sample tilt angle. Domain images were obtained in the hollow square sample. Observed domain images when magnetized to TD are shown in figure 10. Zigzag shape domains called "saw-tooth" patterns appear intersecting main domains [12]. The saw-tooth patterns are thought to have the inner domain structures as illustrated in figure 11-(A). At higher flux density, domain structures

called “column patterns” appear as illustrated in figure 11-(B). In these structures, magnetic flux to TD is conveyed by the transverse domains, and flux density B should be proportional to the volume fraction of these transverse domains and formulated as $B = B_s v_T \cos(\pi/4)$, where: B_s – saturation flux density, v_T – transverse domain volume fraction. Transverse domains are elongated by $3/2\lambda_{100}$ to $\langle 100 \rangle$ -directions at the angle of 45-degrees to the surface and elongated by $3/2\lambda_{100}\cos(\pi/4)$ to TD. From these formulations, magnetostrictive elongation to TD is described with equation (1).

$$(1) \quad \lambda = \frac{3}{2} \lambda_{100} \frac{B}{B_s} \cos \frac{\pi}{4}$$

where: λ – magnetostriction to TD, B – flux density, B_s – saturation flux density.

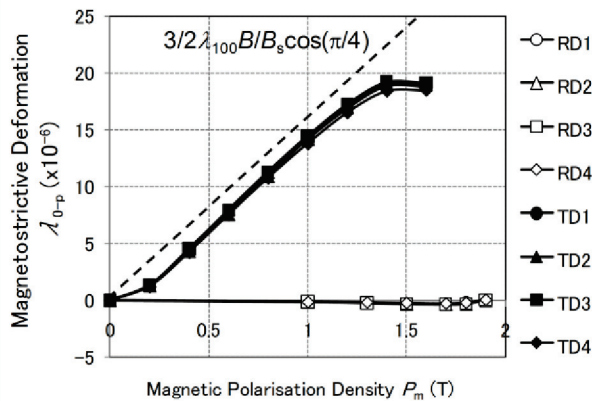


Fig.12. Measured magnetostriction 0- peak values of high permeability GO to RD and TD.

This formulation was compared with measured data. In figure 12, magnetostrictions at peak flux density are plotted as a function of peak flux densities. The dotted line describes the relation of equation (1) and shows a considerably good agreement with the measured magnetostrictions when magnetized to TD. It is realized that TD-magnetostrictions are well described by the domain model shown above.

The small contraction of TD-magnetostrictions from the equation at higher flux density could be explained as follows. At higher flux density above $B_s \cos(\pi/4)$, flux density cannot be increased by the increase of transverse domain volume fraction v_T , and the rotation of magnetizations from $\langle 100 \rangle$ -directions should occur. Saturation magnetostrictions to directions out of $\langle 100 \rangle$ -directions somehow differ from those to $\langle 100 \rangle$ -directions, and this may cause some contractions at higher flux density.

As mentioned above, magnetostriction to TD is almost two-order larger than that to RD. TD-magnetized area in a transformer core should be reduced to decrease the transformer noise, as well as magnetostriction to RD should be reduced. Magnetostriction to TD is determined by the volume fraction of transverse domain fraction and is proportional to TD magnetization. Magnetic flux distribution around T-joint to minimize TD-magnetized area would be the novel solution for transformer noise reduction.

Conclusions

1. Magnetostrictions to RD of high permeability GO sheets are usually small and well described by the domain models considering lancet behaviors, qualitatively.
2. Magnetostrictions to TD of high permeability GO sheets are almost two-order larger than those to RD and well described by the domain models considering transverse domains, quantitatively.

REFERENCES

- [1] Enokizono M., Takahashi K., Yamamura Y., Development of a new strain gauge for measurement of two-dimensional magnetostriction, *J. Magn. Magn. Matr.*, 196-197 (1999) 907-909
- [2] Hirano M., Ishihara Y., Harada K., Todaka T., A study on measurement of magnetostriction of silicon steel sheet by laser displacement meter, *J. Magn. Magn. Matr.*, 254-255 (2003) 43-46
- [3] Anderson P.I., Moses A.J., Stunbury H.J., Assessment of the stress sensitivity of magnetostriction in grain oriented silicon steel, *IEEE Trans. Magn.*, 43 (2007) No.8, 3467-3475
- [4] Yamaguchi H., Pfützner H., Hasenzagl A., Magnetostriction measurement on the multidimensional magnetization performance of SiFe steel, *J. Magn. Magn. Matr.*, 320 (2008) 618-622
- [5] Yabumoto M., Arai S., Kawamata R., Mizokami M., Kubota T., *J. Matr. Eng. Perf.*, 6 (1997) 713-721
- [6] Tsuno K, *Rev. Sol. Stat. Sci.*, 2 (1988) No.4, 623-658
- [7] Allia P., Ferro-Milone A., Montaleni G., Soardo G.P., Vinai F., Theory of negative magnetostriction in grain oriented 3% SiFe for various inductions and applied stresses, *IEEE-Trans. Magn.*, MAG-14 (1978) No.5, 362-364
- [8] Hubert A., Heinicke W., Kranz J., *Zeit. angew. Phys.*, 29 (1965) No. 6, 521-529
- [9] Arakawa E., Maruyama K., Mori K., Nishigaitsu H., Aizawa N., Magnetostriction observed by X-ray diffraction in iron, *IEEE Trans. Magn.*, 41 (2005) No.10, 3718-3720
- [10] Baer N., Hubert A., Jillek W., *J. Magn. Magn. Matr.*, Quantitative investigation into supplementary domain structure of misoriented grains of transformer steel, 6 (1977) 242-248
- [11] Yamamoto T, Nozawa T, Effect of tensile stress on total loss of single crystals of 3% silicon iron, *J. Appl. Phys.*, 41 (1970) No.7, 2981-2984
- [12] Hubert A, *Z. angew. Phys.*, 18 (1965) Heft 5-6, 474-479

Authors: Satoshi Arai, Electromagnetic Materials Laboratory, Nippon Steel Corporation, Shintomi 20-1, 293-8511 Futtsu, Japan, E-mail: arai.satoshi@nsc.co.jp, dr. Masato Mizokami, E-mail: mizokami.masato@nsc.co.jp, dr. Masao Yabumoto, E-mail: yabumoto.masao@nsc.co.jp